2013

Analysis of subcellular [57Co] cobalamin distribution in SH-SY5Y neurons and brain tissue

Hua Zhao
University of Wollongong, hz739@uowmail.edu.au

Kalani Ruberu
University of Wollongong, kalani@uow.edu.au

Hongyun Li
University of Wollongong, hongyun@uow.edu.au

Brett Garner
University of Wollongong, brettg@uow.edu.au

Publication Details

Zhao, H., Ruberu, K., Li, H. & Garner, B. (2013). Analysis of subcellular [^{57}Co] cobalamin distribution in SH-SY5Y neurons and brain tissue. Journal of Neuroscience Methods, 217 (1-2), 67-74.

Analysis of subcellular [57Co] cobalamin distribution in SH-SY5Y neurons and brain tissue

Abstract
Cobalamin (Cbl) utilization as a cofactor for methionine synthase and methylmalonyl-CoA mutase is dependent on the transport of Cbl through lysosomes and its subsequent delivery to the cytosol and mitochondria. We speculated that neuropathological conditions that impair lysosomal function (e.g., age-related lipofuscinosis and specific neurodegenerative diseases) might impair lysosomal Cbl transport. To address this question, an appropriate method to quantify intracellular Cbl transport in neuronal cell types and brain tissue is required. Thus, we developed methods to measure [^{57}Co] Cbl levels in lysosomes, mitochondria and cytosol obtained from in vitro and in vivo sources. Human SH-SY5Y neurons or HT1080 fibroblasts were labeled with [^{57}Co] Cbl and homogenized using a ball-bearing homogenizer, and the lysates were separated into 10 fractions using ultracentrifugation in an OptiPrep density gradient. Lysosomes were recovered from the top of the gradient (fractions 1-5), which were clearly separated from mitochondria (fractions 7-9) on the basis of the expression of the marker proteins, LAMP2 and VDAC1. The isolated lysosomes were intact based on their colocalization with acid phosphatase activity. The lysosomal and mitochondrial fractions were free of the cytosolic markers beta-actin and methionine synthase. The relative distribution of [^{57}Co] Cbl in both neurons and fibroblasts was as follows: 6% in the lysosomes, 14% in the mitochondria and 80% in the cytosol. This technique was also used to fractionate organelles from mouse brain, where marker proteins were detected in the gradient at positions similar to those observed for the cell lines, and the relative distribution of [^{57}Co] Cbl was as follows: 12% in the lysosomes, 15% in the mitochondria and 73% in the cytosol. These methods provide a useful tool for the investigation of intracellular Cbl trafficking in a neurobiological setting.

Keywords
57co, cobalamin, distribution, sh, subcellular, sy5y, analysis, neurons, brain, tissue

Disciplines
Medicine and Health Sciences

Publication Details
Zhao, H., Ruberu, K., Li, H. & Garner, B. (2013). Analysis of subcellular [^{57}Co] cobalamin distribution in SH-SY5Y neurons and brain tissue. Journal of Neuroscience Methods, 217 (1-2), 67-74.

Analysis of subcellular [^{57}Co]cobalamin distribution in SH-SY5Y neurons and brain tissue

Hua Zhao[a,b], Kalani Ruberu[a,b], Hongyun Li[a,b] and Brett Garner[a,b,*]

[a]Illawarra Health and Medical Research Institute, University of Wollongong, NSW 2522, Australia; [d]School of Biological Sciences, University of Wollongong, NSW 2522, Australia.

Key words: lysosome, mitochondria, cobalamin, subcellular-fractionation, brain, neuron

Number of text pages including tables and figures: 32

Number of figures: 6

Number of tables: 1

* Corresponding author: Professor Brett Garner, School of Biological Sciences, University of Wollongong, NSW 2522, Australia. Tel.: +61-2-4298 1576, Fax. +61-2-4221 8130, Email: brettg@uow.edu.au

Abstract

Cobalamin (Cbl) utilization as a cofactor for methionine synthase and methylmalonyl-CoA mutase is dependent on its transit through lysosomes and subsequent delivery to cytosol and mitochondria. We speculate that neuropathological conditions that impair lysosomal function (e.g. age-related lipofuscinosis and certain neurodegenerative diseases) may impair lysosomal Cbl transport. To study this question, an appropriate method to quantify intracellular Cbl transport in neuronal cell types and brain tissue is required. We therefore developed methods to measure [^{57}Co]Cbl levels in lysosomes, mithochondria and cytosol derived from in vitro and in vivo sources. Human SH-SY5Y neurons or HT1080 fibroblasts were labelled with [^{57}Co]Cbl, homogenised using a ball-bearing homogenizer, and the lysates separated into 10 fractions using ultracentrifugation on an OptiPrep density gradient. Lysosomes were recovered at the top of the gradient (fractions 1 to 5) and were clearly separated from mitochondria (fractions 7 to 9) based on marker proteins LAMP2 and VDAC1, respectively. The isolated lysosomes were intact based on colocalisation with acid phosphatase activity. The lysosomal and mitochondrial fractions were free of cytosolic markers beta-actin and methionine synthase. The relative distribution of [^{57}Co]Cbl in both neurons and fibroblasts was: lysosomes 6%, mitochondria 14% and cytosol 80%. The technique was also used to fractionate organelles from mouse brain where the marker proteins were detected in the gradient at similar positions to the cell lines and relative distribution of [^{57}Co]Cbl was: lysosomes 12%, mitochondria 15% and cytosol 73%. These methods provide a useful tool for investigating intracellular Cbl trafficking in a neurobiology setting.

[1]*Abbreviations*: AdoCbl, adenosyl cobalamin; Cbl, cobalamin, Hcy, homocysteine; LAMP2, lysosomal-associated membrane protein 2; LER, Lysosome Enrichment Reagent; Met, methionine; MS, methionine synthase; MeCbl, methyl Cbl; MMCM, methylmalonyl-coenzyme A mutase; 5-methyl-THF, 5-methyltetrahydrofolate; THF, tetrahydrofolate; VDAC1, voltage-dependent anion channel 1.

1. Introduction

Cobalamin (Cbl)[1] is required for erythrocyte formation and DNA synthesis, and plays a crucial role in the maintenance of neurological function. Methyl Cbl (MeCbl) and adenosyl Cbl (AdoCbl) are the forms that are active in human metabolism. These two forms of Cbl differ only in the functional group attached to the Co atom at the centre of the Cbl corrin ring. MeCbl is used to transform homocysteine (Hcy) to methionine (Met) via cytosolic methionine synthase (MS). This reaction requires donation of a methyl group derived from the transformation of 5-methyltetrahydrofolate (5-methyl-THF) to tetrahydrofolate (THF). Through the action of methionine adenosyltransferase, Met is utilized in the formation of S-adenosylmethionine (SAM), a universal methyl donor for numerous substrates, including DNA, RNA, hormones, proteins, and lipids. AdoCbl is required for the conversion of methylmalonyl-coenzyme A (Mm-CoA) to succinyl-coenzyme A (Succ-CoA) via mitochondrial Mm-CoA mutase (MMCM). Succ-CoA then enters the Krebs cycle, after which it may be utilized in many pathways including conversion to succinate which may be used as an electron donor or in the synthesis of porphyrins such as haeme.

MS and MMCM activities are reduced in human Cbl deficiency states, causing increased tissue and plasma Hcy levels and, subsequent to the conversion of Mm-CoA to methylmalonic acid (MMA), increased tissue and plasma MMA levels. Because of the roles of both MS and MMCM in methylation reactions and multiple pathways related to, for example, amino acid and lipid metabolism, the clinical Cbl deficiency phenotypes are multifaceted (Baik and Russell, 1999). In addition to the "loss of function" caused by impaired MS and MMCM activities, the accumulation of Hcy and MMA is neurotoxic and is thought to contribute to neurodegeneration and loss of cognitive capacity (Kolker et al., 2000; Morris, 2003).

Cbl utilization is dependent on its transit through the intracellular lysosomal compartment (Banerjee et al., 2009; Gailus et al., 2010; Zhao et al., 2011). We have recently proposed that pathophysiological impairment of lysosomal functions that occur in various conditions such as Alzheimer's disease, lysosomal storage disorders and in age-related neuronal lipofuscinosis may form a "road block" for efficient Cbl utilization in cells. We predict that these conditions may impair the release Cbl from its carrier protein transcobalamin-II (TCII) and inhibit the transport of lysosomal Cbl to both MS and MMCM (Zhao et al., 2011). In addition, it is known that the acidic pH of the lysosome also influences the conversion of Cbl from the "base-on" to "base-off" state, which refers to the interaction of the dimethylbenzimidazole moiety of the Cbl molecule with the central Co atom (Banerjee, 2006). The Cbl base-off state is thought to be important for subsequent interactions with cytosolic cargo proteins.

In order to accurately assess the trafficking of Cbl through the lysosomal compartment it is necessary to establish subcellular fractionation methods that clearly separate lysosomes from the intracellular compartments that contain MS and MMCM, i.e. the cytosol and mitochondria, respectively. The aim of the current experiments was therefore to develop subcellular fractionation methods whereby cells and brain tissues could be metabolically labeled with [^{57}Co]Cbl in order to quantify Cbl distribution between lysosomes, mitochondria and cytosol.

2. Materials and methods

2.1. Cell culture

Experiments were performed using human neuroblastoma cells (SH-SY5Y, ATCC #CRL-2266) and human fibrosarcoma cells (HT1080, ATCC #CCL-121) obtained from the American Type Culture Collection (ATCC, Manassas, VA, USA). Cells were cultured in DMEM supplemented with 10% fetal calf serum, 1% penicillin/streptomycin, and 1% glutamine, at 37˚C in a humidified atmosphere containing 5% CO_2. Cells were grown in four 175 cm^2 plastic flasks until approximately 70% confluent, when cells were incubated with [^{57}Co]cyanoCbl (0.025 μCi/ml; Cat. No. 06B-430002, MP Biomedicals, USA) in DMEM with 10% human serum and 1% penicillin/streptomycin and 1% glutamine for 48 h. The cells were then rinsed with cold (10˚C) PBS and harvested with 1% trypsin, and centrifuged at 600 *g* for 5 min at 4˚C. A small portion of the cells was stained with 0.5% trypan blue to determine the number of viable cells.

2.2. Cell homogenization

A lysosome enrichment kit (Pierce, Cat #89839, USA) was applied to perform subcellular fractionation. An 800 μl aliquot of extraction buffer Lysosome Enrichment Reagent (LER) "A" containing 1% protease inhibitors was added to the cell pellets. The pellets were gently re-suspended and incubated on ice for no more than 2 minutes. The cell suspension was transferred to a ball-bearing cell homogenizer (Isobiotec, Germany) and homogenized on ice. To check lysis efficiency, 10 μl of cell lysate was stained with 0.5% trypan blue and viewed under a light microscope. Homogenization was continued until 95% cell membrane breakage was achieved (typically 10 to 15 passages through the homogenizer). Next, the lysed cells were transferred into a 2 ml microcentrifuge tube and 800 μl of LER "B" containing 1% protease inhibitors was mixed with the lysed cells. The mixed cell lysates were centrifuged at

600 *g* for 10 min at 4˚C to remove nuclei and membranous debris and the supernatant (1500 μl) containing lysosomes, mitochondria and cytosol was collected.

2.3. Density gradient ultracentrifugation

To prepare a discontinuous density gradient, five gradient solutions were prepared by mixing gradient dilution buffer (a 1:1 mixture of LER A and LER B) with the OptiPrep medium (that is supplied as a 60% solution in H_2O) as described in Table 1. The diluted OptiPrep density gradient solutions were carefully overlayed in descending concentration order (i.e. 30% OptiPrep solution first and then 27%, 23%, 20% and 17%) in a 7 ml ultracentrifuge tube (Hitachi Koki, Japan). Next, the prepared 1500 μl supernatants from the cell extracts described above were mixed with 500 μl of OptiPrep medium to make a final concentration of 15% OptiPrep and this was overlayed on the top of the density gradient. The tube was centrifuged at 145,000 *g* for 4 h at 4˚C using a Sorvall MTX 150 ultracentrifuge and a Sorvall S50ST swinging bucket rotor (Thermo Scientific). After centrifugation, two distinct bands appeared in the gradient solution (Fig. 1).

A total of 10 fractions of 600 μl each were carefully withdrawn from the top of the gradients using extra long micropipette tips (Finntip 200, Thermo Scientific). The amount of [^{57}Co]Cbl in each fraction was measured by a Wallace Gamma Counter (PerkinElmer, Finland). Next, each isolated fraction was mixed with 1000 μl PBS and centrifuged at 20,000 *g* for 30 min at 4˚C to separate lysosomes and mitochondria from cytosol. After centrifugation, the supernatant of each fraction was collected and labeled as cytosolic fractions; while the pellets from each fraction were mixed with 400 μl PBS and labeled as lysosomal and mitochondrial fractions (subsequent to identification of organelle markers by western blotting as described

below). Both the pellet and supernatant fractions were assessed for [^{57}Co]Cbl radioactivity and organelle markers. An overview of the procedure is illustrated in Figure 1.

2.4. Western blotting

To identify the fractions containing lysosomes, mitochondria, and cytosol, western blotting was performed with appropriate antibodies to marker proteins; lysosome, lysosomal-associated membrane protein 2 (LAMP2, Southern Biotech); mitochondria, voltage-dependent anion channel 1 (VDAC1, Abcam); cytosol, β-actin (Sigma) and methionine synthase / 5-methyltetrahydrofolate-homocysteine methyltransferase (MS, Abnova). Briefly, sample proteins from each fraction were separated on 12% SDS PAGE gels using a Mini-Protean II system (Bio-Rad) at 150 V for 70 minutes followed by transfer at 100 V for 30 min onto 0.45 μm nitrocellulose membranes using a Mini-Trans-Blot Electrophorectic Transfer cell (Bio-Rad). The membranes were blocked in 5% (w/v) non-fat milk powder in PBS for 1 h at 22˚C and then probed with anti-LAMP2 mouse monoclonal antibody (1:4000), anti-VDAC1 rabbit polyclonal antibody (1:4000), anti-β-actin rabbit polyclonal antibody (1:10000), and anti-MS goat polyclonal antibody (1:300) at 4°C for 16 h, followed by incubation with the appropriate horseradish-peroxidase-conjugated rabbit anti-mouse (1:4000, Dako), goat anti-rabbit (1:4000, Dako), and rabbit anti-goat (1:4000, Dako) IgG antibodies for 1 h at 22˚C. Blots were rinsed in PBS and proteins were detected using enhanced chemiluminescence (ECL, Amersham Biosciences). The membranes were exposed to X-ray film (Fuji), developed, scanned and signal intensity was quantified using NIH Image software.

2.5. Acid phosphatase assay

During cell homogenization and ultracentrifugation, lysosome membranes are susceptible to pressure and may be broken, thus lysosomal hydrolases may be leaked into the cytosol as a consequence. Acid phosphatase is one of the acid hydrolases that exist in lysosomes and therefore is a classical marker for the identification of lysosomes in subcellular fractionation studies. The acid phosphatase assay kit (Sigma, Cat #CS0740) was applied to detect lysosome membrane integrity in each fraction. Briefly, a substrate solution was prepared by dissolving one 4-nitrophenyl phosphate tablet in 5 ml of citrate buffer and the solution equilibrated at 37˚C. The standard solution was prepared by diluting 5 µl of the 10 mM nitrophenol standard solution in 995 µl of 0.5 M NaOH. The reaction components and samples were added to 96-well microtitre plates according to the manufacturer's instructions and samples analysed in triplicate. The plate was incubated for 10 min at 37˚C after which time 200 µl of 0.5 M NaOH was added to all wells (except the standard) to stop the reaction. Absorption was measured at 405 nm using a microtitre plate reader (Spectra Max, Bio Strategy) and results expressed as acid phosphatase Units / ml (where 1 Unit of enzyme activity will hydrolyse 1 µmole of 4-nitrophenyl phosphate per min at pH 4.8 at 37˚C).

2.6. Animal study

To examine the subcellar distribution of [^{57}Co]Cbl in lysosomes, mitochondria, and cytosol derived from the brain, an *in vivo* study was carried out using two 12-month old male wild-type C57Bl/6J mouse. This study was approved by the University of Wollongong Animal Ethics Committee and was carried out in accordance with EU Directive 2010/63/EU for animal experiments. The mice were intraperitoneally injected with 4 µCi [^{57}Co]cyanoCbl in a volume of 0.2 ml sterile saline (0.9% w/v NaCl). The mice were weighed at time of injection

and again just before sacrifice. After 72 h the mice were sacrificed and the blood samples were collected by cardiac puncture. The mice were then transcardially perfused with PBS and the brain, liver and kidney were dissected. All organs were weighed and the amount of [^{57}Co]Cbl in these organs was measured using a gamma counter. In this experiment, only the brain was used for organelle isolation. The brain was rinsed with PBS and cut into small pieces (< 3 mm^3). The procedures for homogenization and subcellular fractionation were the same as described above for cultured cells.

2.7. Data analysis

Data are presented as mean ± SE of three independent experiments unless stated otherwise. Note that the results for [^{57}Co]Cbl are presented as counts per minute (cpm). The radioactive tracer molecule [^{57}Co]cyanoCbl was provided by the supplier in batches of 10.5 μCi in a volume of 1 ml H_2O containing 0.9% (vol/vol) benzyl alcohol. On the reference date provided by the manufacturer, 0.1 ml from each batch of [^{57}Co]cyanoCbl yielded 2.0 x 10^6 cpm. After evaporation to dryness and reconstitution in cell culture medium (or saline for i.p. injection), the [^{57}Co]cyanoCbl radioactivity was measured in a 0.1 ml aliquot to confirm radioactivity before use in all experiments. For the experiments described herein, the [^{57}Co]cyanoCbl tracer was routinely used within 2 months of the reference date and the radioactivity per 0.1 ml on the day of preparation for addition to cells or animals was 1.52 x 10^6 $\pm$ 0.04 x 10^6 cpm (mean $\pm$ SE, n = 8). The values ranged form 1.37 x 10^6 - 1.65 x 10^6 cpm in these experiments. As an approximation, based on a specific activity for [^{57}Co]cyanoCbl of 300 μCi / μg, at the time of use in experiments 1000 cpm equates to ~ 2.4 pg of [^{57}Co]Cbl. It should be noted that in two months the radioactivity of ^{57}Co has decreased by 14% and this needs to be taken into account when comparing values.

3. Results

3.1. Method overview

Cbl exists in three main compartments in the cell: the lysosome, mitochondria and cytosol. In order to accurately assess Cbl transit through intracellular compartments, it is essential to develop methods that can separate at least these three compartments into fractions in which labeled Cbl can be unambiguously quantified. We therefore used the following steps to achieve this: (1) cells were labeled with [^{57}Co]Cbl; (2) cells were disrupted in a ball-bearing homegnizer, (3) the isolated organelles were separated from cellular membrane debris and nuclei, (4) the organelles were separated over an OptiPrep density gradient by ultracentrifugation, (5) ten fractions were collected from the gradient, and (6) the fractions were separated into pellet (organelle) and supernatant (cytosol) fractions. The methodological detail for each of these steps is described in "Materials and Methods" and an overview is illustrated in Figure 1. The purified fractions were then analysed for various organelle markers and for [^{57}Co] radioactivity.

3.2. Isolation of lysosomes, mitochondria and cytosol from fibroblasts

Our initial experiments focused on the HT1080 human fibroblast cell line. Western blot analysis of the organelle fractions for LAMP2 and VDAC1 (lysosomal and mitochondrial markers, respectively) revealed lysosomes were recovered from the top of the OptiPrep gradient, especially in Fraction 1 (Fig. 2A). As LAMP2 was also detected at lower levels in Fractions 2 to 5, these fractions together (Fractions 1 to 5) were considered to represent the lysosomal content of the cells. In contrast, VDAC1 was detected in Fractions 7 to 9 and thus

represented the mitochondrial fractions. It is noteworthy that β-actin was detected at very low levels, if at all, in the isolated organelle fractions, and MS was not detected in any of the organelle fractions (Fig. 2A). This indicates that pure lysosomes can be separated from mitochondria and that both organelles are essentially free of cytosolic contaminants that may spuriously contribute to apparent organelle Cbl levels.

The cytosolic components of each of the ten OpitPrep gradient fractions were also assessed by western blotting. Neither LAMP2 nor VDAC1 were detected in the cytosolic fractions, whereas β-actin was clearly detected in Fractions 1 to 8, with particularly high levels in Fractions 1 to 4 (Fig. 2B). In addition, MS was detected in Fractions 1 to 3, with particularly high levels in Fraction 2.

3.3. Isolation of lysosomes, mitochondria and cytosol from neurons

We also used the same method to purify lysosomes and mitochondria from the human SH-SY5Y neuronal cell line. Similar to the results derived from our fibroblast studies, pure lysosomal and mitochondrial preparations were recovered from Fractions 1 to 5 and from Fractions 7 to 9, respectively (Fig. 3A). Neither β-actin nor MS were detected in the organelle fractions (Fig 3A). Assessment of the cytosolic fractions revealed there was no contamination of cytosol with lysosomes or mitochondria, as assessed by lack of signal for LAMP2 and VDAC1, respectively (Fig. 3B). Moreover, β-actin was clearly detected in Fractions 1 to 9, with particularly high levels in Fractions 1 to 6, whereas MS was detected in predominantly Fractions 2 to 5 (Fig. 3B).

The methods we describe can therefore be used to isolate pure lysosomal, mitochondrial and cytosolic preparations from fibroblasts and neurons.

3.4. Confirmation that isolated lysosomes remain intact after purification

To confirm that the isolated lysosomes remained intact during the homogenization and ultracentrifugation procedures, we assessed all organelle and cytosolic fractions for acid phosphatase activity. The data indicate that acid phosphatase activity correlated with the expression of LAMP2 in the lysosomal fractions from both fibroblasts and neurons (Fig 4A and 4B, respectively). Furthermore, acid phosphatase activity was not detected in any of the cytosolic fractions (Fig 4). This indicates that lysosomes remain structurally intact during the isolation procedures and that the lysosomal membranes are not compromised. Note that the buffers used in the acid phosphatase assay were adjusted to pH 4.8 so that even if the enzyme was located in the cytosol (normally close to neutral pH) we would still detect its activity in the 4-nitrophenyl phosphate hydrolysis assay.

3.5. Subcellular [^{57}Co]cobalamin distribution in fibroblasts and neurons

Having established methods for the isolation of pure lysosomes, mitochondria and cytosol, and shown that the lysosomes maintain their structural integrity, we next assessed the subcellular distribution of [^{57}Co]Cbl in the both fibroblasts and neurons subsequent to metabolic radiolabeling.

Our pilot studies indicated that [^{57}Co]Cbl labeling required 0.025 μCi [^{57}Co] / ml of growth medium for a 48 h incubation period. We observed that the use of either bovine serum or heat-inactivated human serum substantially reduced the incorporation of [^{57}Co]Cbl into cells (H. Zhao and B. Garner, unpublished observations). After the 48 h labeling period, 24.2 $\pm$

1.3% of the radioactivity was incorporated into the fibroblasts (mean ± SE, n=3). Interestingly, under the same culture conditions only 6.9 ± 1.5% of the radioactivity was incorporated into the neurons (mean ± SE, n=3). Despite the relatively low level of isotope incorporation, this was clearly sufficient to assess [^{57}Co]Cbl distribution in lysosomes, mitochondria and cytosol. The data presented in Figure 5A indicate that for fibroblasts, the relative distribution of [^{57}Co]Cbl was: lysosomes 5.8 ± 0.2%, mitochondria 14.0 ± 0.7% and cytosol 80.2 ± 0.9% (all mean ± SE, n=3). The corresponding data for neurons was: lysosomes 5.1 ± 0.3%, mitochondria 13.3 ± 0.6% and cytosol 81.6 ± 0.8% (all mean ± SE, n=3). Even though we observed a degree of variability in the absolute CPM values for [^{57}Co]Cbl in each of the fractions assessed over three independent experiments (Fig 5B), the proportional distribution of [^{57}Co]Cbl in the intracellular compartments was remarkably constant (Fig 5A).

3.6. Subcellular [^{57}Co]cobalamin distribution in lysosomes, mitochondria and cytosol from brain

In a final series of experiments, we assessed if the subcellular fractionation methods utilized above could also be applied to study [^{57}Co]Cbl distribution in lysosomes, mitochondria and cytosol isolated from mouse brain. Two male C57Bl/6J mice were injected intraperitoneally with 3 μCi [^{57}Co]Cbl. After 72 h the mice were euthanased, perfused with PBS, and the major organs (listed below) were carefully dissected. The distribution of radioactivity in the whole organs collected from the two mice was: brain 13,200 – 14,000 cpm, liver 354,000 - 412,000 cpm, kidney 316,000 – 545,000 cpm, heart 8,100 – 8,500, spleen 11,000 – 14,600 cpm (individual values shown, n=2). The radioactivity in plasma was 117,000 – 128,000 cpm per 100 μl (individual values shown, n=2), and in faeces was 340,000 cpm (total value and

only collected in one experiment). A total of 32% of the injected [^{57}Co]Cbl radioactivity was recovered in these samples. The relative ratio of [^{57}Co]Cbl recovered in the whole organs was: brain 1 : liver 28 : kidney 32 : heart 0.6 : spleen 1.

We then subjected the whole brain to the subcellular fractionation method developed above. Highly purified lysosomal and mitochondrial preparations that were essentially free of β-actin were recovered from Fractions 1 to 4 and from Fractions 7 to 9, respectively (Fig. 6A). Analysis of the mouse brain cytosolic fractions indicated a strong signal for β-actin in Fractions 1 to 5 and no contamination with either LAMP2 or VDAC1 (Fig. 6B). Similar to the data derived from cultured cells, acid phosphatase activity colocalised predominatly in the LAMP2-positive fractions (Fig. 6C). Finally, the relative distribution of [^{57}Co]Cbl in the organelle fractions derived from the brain was measured and found to be: lysosomes 215 (5) cpm, mitochondria 290 (25) cpm and cytosol 1295 (35) cpm (mean values with range shown in parentheses). The corresponding relative percentage distribution values were therefore lysosomes 12%, mitochondria 15%, and cytosol 73% (Fig. 6D).

4. Discussion

In the present work we have successfully developed a [^{57}Co]Cbl metabolic labeling / subcellular fractionation method that permits the separation of the two major pools of intracellular Cbl (in the cytosol and mitochondria) from the presumably more transient lysosomal pool. This methodology builds on many previous studies that have separately analysed cellular [^{57}Co]Cbl metabolism in cells and mice (Hannibal et al., 2008; Mellman et al., 1978; Yamani et al., 2008; Yassin et al., 2000; Youngdahl-Turner et al., 1978) or aspects of lysosome function in cells and mice (Manunta et al., 2007; Yang et al., 2011). Our data

derived from fibroblast and neuronal cell lines indicates that under steady-state conditions, only ~6% of cellular [^{57}Co]Cbl resides in the lysosome. This is perhaps not surprising based on the fact that the major sites of Cbl utilization in humans are the enzymes MS and MMCM located in the mitochondria and cytosol respectively. We also showed that the subcellular fractionation methods could be used to assess lysosomal [^{57}Co]Cbl content in mouse brain. In this case ~12% of cellular [^{57}Co]Cbl was detected in the lysosome and this was similar to the amount in mitochondria (~15%). It is currently not clear why lysosomes isolated from the brain are apparently enriched in [^{57}Co]Cbl as compared to the cell lines. We were unable to measure mouse MS by western blotting so it is possible that traces of cytosolic contamination in these fractions could contribute to the cpm values; although the very low levels of β-actin contamination would argue against this. Further rinse steps after the OptiPrep gradient (see Fig 1) may improve organelle purity; however, the challenge with the brain analysis is the relatively low amount of [^{57}Co]Cbl incorporation and the possibility that further rinsing may reduce recovery of the lysosomes. In the brain subcellular fractionation experiments, much more material was loaded onto the OptiPrep gradient (e.g. the lysosomal acid phosphatase activity is 10-fold higher than for the neuronal cell line (compare Fig. 3B and Fig. 6C) and it is possible that analysis of a smaller fraction of the brain tissue would alter the recovery of organelles through the fractions. Again, though, this would reduce the amount of [^{57}Co]Cbl that could be detected in the fractions. Future studies could adapt the methods we have established to investigate lysosomal [^{57}Co]Cbl distribution in brain tissues from other species and in mouse models of ageing and neurodegenerative disease.

We also noted that in the subcellular fractionation of the brain tissue, a small increase in acid phosphatase activity was present with the major mitochondrial fraction (Fraction 8). We did not detect LAMP2 in this fraction so lysosomal contamination seems unlikely. One possible

explanation could be that one or more of the several known mitochondrial phosphatases may have residual activity at pH 4.8 and thus act upon the 4-NPP is our assay (McBride et al., 2006).

The critical role that the lysosome plays in delivery of Cbl to MS in the cytosol and MMCM in the mitochondrion is demonstrated by the inborn error of Cbl metabolism referred to as *cbl*F. This life-threatening condition is caused by defects in the *LMBRD1* gene that encodes LMBD1 (Rutsch et al., 2009). The defect in lysosomal Cbl release was discovered 25 years ago, well before the likely transporter involved was characterised (Rosenblatt et al., 1985). These pioneering studies also showed that chloroquine, a compound that increases lysosomal pH above its physiological level of ~ 4.5 thereby inhibiting lysosomal protease activity, prevents the release of Cbl from TCII and blocks the transport of lysosomal [^{57}Co]Cbl to both MS and MMCM (Rosenblatt et al., 1985). We have recently hypothesized that in addition to *LMBRD1* mutations and drug-mediated alterations of lysosomal function that may trap Cbl in the lysosome, additional pathophysiological perturbations in lysosome function could also represent a "roadblock" for Cbl transit through the lysosomal compartment (Zhao et al., 2011). Future studies could utilize the methods we have established herein to assess cell lines and animals models that are known to have impaired lysosome function due to, for example, accumulation of the age pigment lipofuscin, substrate accumulation in various lysosomal storage diseases, or accumulation of β-amyloid (Zhao et al., 2011). Based on the fact that Cbl deficiency includes a neurological phenotype (Baik and Russell, 1999; Calvaresi and Bryan, 2001; Healton et al., 1991) we focused on brain tissue in the *in vivo* aspect of the present study. There is no reason why the techniques could not be employed to study other tissues in animal studies and we predict (based on the much higher [^{57}Co]Cbl levels recovered in the liver and kidney, that the injected [^{57}Co]Cbl dose could be reduced at least 10-fold. Finally,

although we have chosen to use commercially available reagents for some of the subcellular fractionation steps, it is likely that buffer compositions that have been published (e.g. (Graham, 2001; Koenig, 1974; Yamada et al., 1984)) may yield similar results.

5. Conclusions

We have established a subcellular fractionation method that provides a useful tool for investigating intracellular [^{57}Co]Cbl trafficking. The method can be applied to both neuronal and fibroblast cell lines and in brain tissues and may be adapted to study the impact that pathophysiological impairment of lysosomal function has on intracellular [^{57}Co]Cbl transport *in vitro* and *in vivo*.

Acknowledgements

We are very grateful for advice from Dr David Watkins and Prof David Rosenblatt (McGill University, Montreal) and Prof Donald Jacobsen (Case Western Reserve University) regarding [^{57}Co]Cbl metabolic labeling, and from Prof Ana Maria Cuervo (Albert Einstein College of Medicine) and Prof Ralph Nixon (Nathan Kline Institute) regarding cell and tissue subcellular fractionation. BG is supported by a Fellowship from the Australian Research Council (ARC Future Fellowship FT0991986).

References

Baik HW, Russell RM. Vitamin B12 deficiency in the elderly. Annu Rev Nutr, 1999; 19: 357-77.

Banerjee R. B12 trafficking in mammals: A for coenzyme escort service. ACS Chem Biol, 2006; 1: 149-59.

Banerjee R, Gherasim C, Padovani D. The tinker, tailor, soldier in intracellular B12 trafficking. Curr Opin Chem Biol, 2009; 13: 484-91.

Calvaresi E, Bryan J. B vitamins, cognition, and aging: a review. J Gerontol B Psychol Sci Soc Sci, 2001; 56: P327-39.

Gailus S, Hohne W, Gasnier B, Nurnberg P, Fowler B, Rutsch F. Insights into lysosomal cobalamin trafficking: lessons learned from cblF disease. J Mol Med, 2010; 88: 459-66.

Graham JM. Isolation of lysosomes from tissues and cells by differential and density gradient centrifugation. Curr Protoc Cell Biol, 2001; Chapter 3: Unit 3 6.

Hannibal L, Axhemi A, Glushchenko AV, Moreira ES, Brasch NE, Jacobsen DW. Accurate assessment and identification of naturally occurring cellular cobalamins. Clin Chem Lab Med, 2008; 46: 1739-46.

Healton EB, Savage DG, Brust JC, Garrett TJ, Lindenbaum J. Neurologic aspects of cobalamin deficiency. Medicine (Baltimore), 1991; 70: 229-45.

Koenig H. The isolation of lysosomes from brain. Methods Enzymol, 1974; 31: 457-77.

Kolker S, Ahlemeyer B, Krieglstein J, Hoffmann GF. Methylmalonic acid induces excitotoxic neuronal damage in vitro. J Inherit Metab Dis, 2000; 23: 355-8.

Manunta M, Izzo L, Duncan R, Jones AT. Establishment of subcellular fractionation techniques to monitor the intracellular fate of polymer therapeutics II. Identification of endosomal and lysosomal compartments in HepG2 cells combining single-step subcellular fractionation with fluorescent imaging. J Drug Target, 2007; 15: 37-50.

McBride HM, Neuspiel M, Wasiak S. Mitochondria: more than just a powerhouse. Curr Biol, 2006; 16: R551-60.

Mellman I, Willard HF, Rosenberg LE. Cobalamin binding and cobalamin-dependent enzyme activity in normal and mutant human fibroblasts. J Clin Invest, 1978; 62: 952-60.

Morris MS. Homocysteine and Alzheimer's disease. Lancet Neurol, 2003; 2: 425-8.

Rosenblatt DS, Hosack A, Matiaszuk NV, Cooper BA, Laframboise R. Defect in vitamin B12 release from lysosomes: newly described inborn error of vitamin B12 metabolism. Science, 1985; 228: 1319-21.

Rutsch F, Gailus S, Miousse IR, Suormala T, Sagne C, Toliat MR, Nurnberg G, Wittkampf T, Buers I, Sharifi A, Stucki M, Becker C, Baumgartner M, Robenek H, Marquardt T, Hohne W, Gasnier B, Rosenblatt DS, Fowler B, Nurnberg P. Identification of a putative lysosomal cobalamin exporter altered in the cblF defect of vitamin B12 metabolism. Nat Genet, 2009; 41: 234-9.

Yamada H, Hayashi H, Natori Y. A simple procedure for the isolation of highly purified lysosomes from normal rat liver. J Biochem, 1984; 95: 1155-60.

Yamani L, Gibbs BF, Gilfix BM, Watkins D, Hosack A, Rosenblatt DS. Transcobalamin in cultured fibroblasts from patients with inborn errors of vitamin B12 metabolism. Mol Genet Metab, 2008; 95: 104-6.

Yang DS, Stavrides P, Mohan PS, Kaushik S, Kumar A, Ohno M, Schmidt SD, Wesson D, Bandyopadhyay U, Jiang Y, Pawlik M, Peterhoff CM, Yang AJ, Wilson DA, St George-Hyslop P, Westaway D, Mathews PM, Levy E, Cuervo AM, Nixon RA. Reversal of autophagy dysfunction in the TgCRND8 mouse model of Alzheimer's disease ameliorates amyloid pathologies and memory deficits. Brain, 2011; 134: 258-77.

Yassin MS, Ekblom J, Xilinas M, Gottfries CG, Oreland L. Changes in uptake of vitamin B(12) and trace metals in brains of mice treated with clioquinol. J Neurol Sci, 2000; 173: 40-4.

Youngdahl-Turner P, Rosenberg LE, Allen RH. Binding and uptake of transcobalamin II by human fibroblasts. J Clin Invest, 1978; 61: 133-41.

Zhao H, Brunk UT, Garner B. Age-related lysosomal dysfunction: an unrecognized roadblock for cobalamin trafficking? Cell Mol Life Sci, 2011; 68: 3963-9.

Figure legends

Fig. 1. Overview of [^{57}Co]Cbl labelling and subcellular fractionation procedures. Cells were incubated with 0.025 μCi/ml [^{57}Co]cyanoCbl in DMEM with 10% (v/v) human serum at 37˚C for 48 h. The cells were then homogenized in a ball-bearing homogenizer to disrupt the plasma membrane. Membrane debris and nuclei were removed by centrifugation at 600 g for 10 min and the supernatant samples overlayed at the top of an OpitPrep density gradient. After ultracentrifugation at 145,000 *g* for 4 h, a total 10 fractions of 600 μl each were collected and the lysosomal/mitochondrial fractions separated from the cytosol by mixing with PBS followed by further centrifugation at 20,000 *g* for 30 min. The organelle and cytosol fractions were thereafter assessed for appropriate markers and for [^{57}Co] radioactivity.

Fig. 2. Separation of lysosomes, mitochondria, and cytosol in HT1080 fibroblast fractions. Approximately 16 x 10^6 cells were metabolically labelled with [^{57}Co]Cbl for 48 h. The radiolabelled cells were disrupted using a ball-bearing homogeniser and the lysosomes, mitochondria, and cytosol fractions were separated using an OptiPrep gradient. The appearance of the markers LAMP2 (lysosomal), VDAC1 (mitochondrial), β-actin and MS (both cytosolic) were then probed by wester blotting in all fractions (note Fraction 1 is the least dense from the top of the gradient). (A) In the pellet fractions, a clear separation could be seen for lysosomes (fractions 1 to 5) and mitochondria (fractions 7 to 9). Cytosolic markers were either absent or present only at trace amounts. (B) In the supernatant portion of the fractions, lysosomal, mitochondrial markers were not detected, however, strong signals for cytosolic markers β-actin (fractions 1 to 8) and MS (fractions 1 to 2) were detected. Data are representative of three independent experiments.

Fig. 3. Separation of lysosomes, mitochondria, and cytosol in SH-SY5Y neuron fractions. Approximately 16 x 10^6 cells were metabolically labelled with [^{57}Co]Cbl for 48 h. The radiolabelled cells were disrupted using a ball-bearing homogeniser and the lysosomes, mitochondria, and cytosol fractions were separated using an OptiPrep gradient. The appearance of the markers LAMP2 (lysosomal), VDAC1 (mitochondrial), β-actin and MS (both cytosolic) were then probed by wester blotting in all fractions (note fraction 1 is the least dense from the top of the gradient). (A) In the pellet fractions, a clear separation could be seen for lysosomes (fractions 1 to 5) and mitochondria (fractions 7 to 9). Cytosolic markers were absent. (B) In the supernatant portion of the fractions, lysosomal, mitochondrial markers were not detected, however, strong signals for cytosolic markers β-actin (fractions 1 to 8) and MS (fractions 2 to 5) were detected. Data are representative of three independent experiments.

Fig. 4. Acid phosphatase activity in HT1080 fibroblast and SH-SY5Y neuron fractions. Approximately 16 x 10^6 cells were disrupted and fractionated using an OptiPrep gradient as described in the Legend to Fig. 2. Acid phosphatase activity (indicating the presence of lysosomes with an intact membrane) was measured in all pellet fractions (circles) and cytosolic fractions (squares) using 4-nitrophenyl phosphate (4-NPP) as a colorimetric substrate. Acid phosphatase activity in HT1080 fibroblast fractions (A) and SH-SY5Y neuron fractions (B) indicate that lysosomes are predominantly found at the top of the density gradient (fraction 1) and are structurally intact (high acid phosphatase activity). Acid phosphatase activity in the supernatant fractions was negligible.

Fig. 5. Distribution of [^{57}Co]Cbl in lysosomes, mitochondria, and cytosol derived from HT1080 fibroblasts and SH-SY5Y neurons. Approximately 16 x 10^6 cells were metabolically labelled with [^{57}Co]Cbl for 48 h. The radiolabelled cells were disrupted using a ball-bearing homogeniser and the lysosomes, mitochondria, and cytosol fractions were separated using an OptiPrep gradient. (A) The proportional distribution of [^{57}Co]Cbl was assessed using a gamma counter and expressed as a percentage of radioactvoty in each fraction for both cell types. Data are means with SE represented by the error bars (n=3 experiments for each cell type). L, lysosome; M, mitochondria; C, cytosol. (B) The cpm data for each of the fractions in three independent experiments performed for each cell type shown in "A" is provided.

Fig. 6. Isolation and characterisation of lysosomes, mitochondria, and cytosol derived from mouse brain. A 12-month old male C57Bl/6J mouse was injected intraperitoneally with 3 μCi [^{57}Co]Cbl and after 72 h the mouse was euthanased, perfused, and the brain was homogenised using a ball-bearing homogeniser. The lysosomes, mitochondria, and cytosol fractions were then separated using an OptiPrep gradient. (A) In the pellet fractions, a clear separation could be seen for lysosomes (fractions 1 to 3) and mitochondria (fractions 6 – 9) based on LAMP2 and VDAC1 levels, respectively. The cytosolic marker, β-actin, was either absent or present only at trace amounts. (B) In the supernatant portion of the fractions, lysosomal and mitochondrial markers were not detected, however, a strong signal for cytosolic marker β-actin (fractions 1 to 5) was detected. (C) Acid phosphatase activity (indicating the presence of lysosomes with an intact membrane) was measured in all pellet fractions (circles) and cytosolic fractions (squares) using 4-nitrophenyl phosphate (4-NPP) as a colorimetric substrate. Acid phosphatase activity indicates that lysosomes are predominantly found at the top of the density gradient (fraction 1) and are structurally intact (high acid phosphatase activity). Acid phosphatase activity in the supernatant fractions was

negligible. (D) The proportional distribution of [^{57}Co]Cbl was assessed using a gamma counter and expressed as a percentage of radioactivity in each fraction. L, lysosome; M, mitochondria; C, cytosol. Data are representative of two similar experiments.

Table 1: OptiPrep density gradient preparation

OptiPrep medium volume (µl)	Gradient dilution buffer volume (µl)	Final volume (µl)	OptiPrep final concentration (%)
283.3	716.7	1000	17
333.3	666.7	1000	20
191.7	308.3	500	23
450	550	1000	27
500	500	1000	30

Figure 1

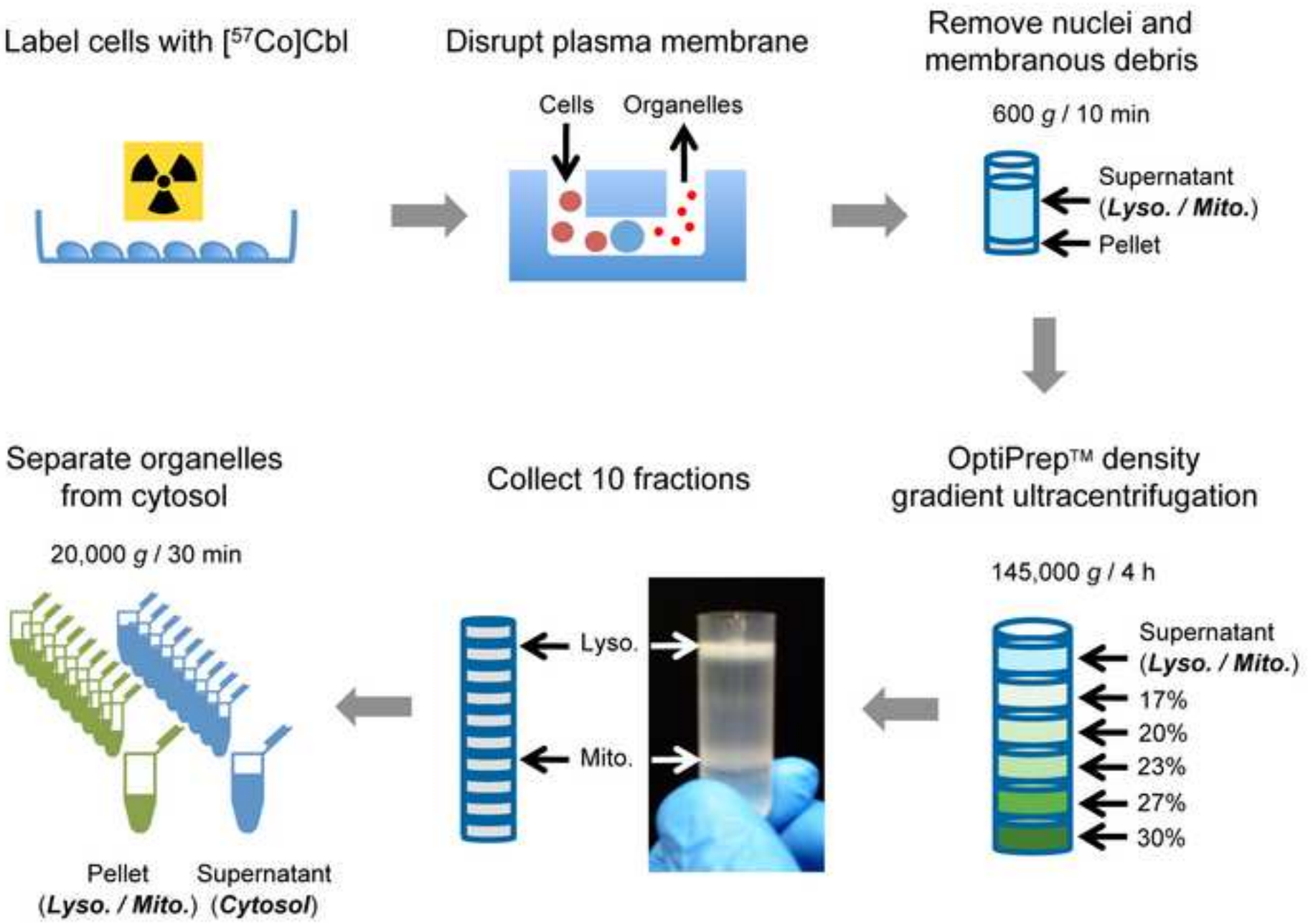
Label cells with [57Co]Cbl
Disrupt plasma membrane
Cells
Organelles
Remove nuclei and membranous debris
600 g / 10 min
Supernatant
(Lyso. / Mito.)
Pellet
OptiPrep™ density gradient ultracentrifugation
145,000 g / 4 h
Supernatant
(Lyso. / Mito.)
17%
20%
23%
27%
30%
Collect 10 fractions
Lyso.
Mito.
Separate organelles from cytosol
20,000 g / 30 min
Pellet
(Lyso. / Mito.)
Supernatant
(Cytosol)

Figure 2

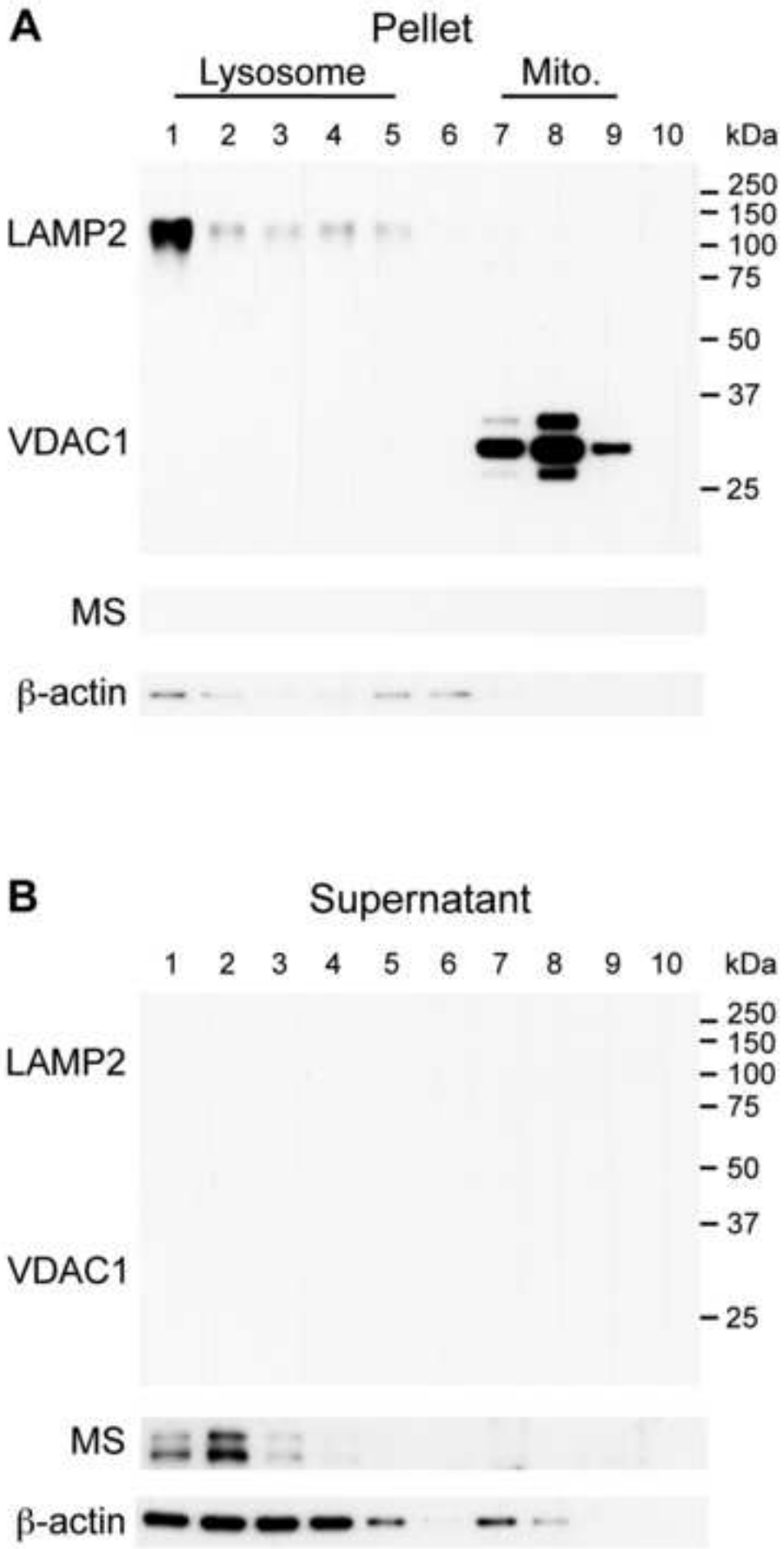
A
Pellet
Lysosome
Mito.
1 2 3 4 5 6 7 8 9 10 kDa
LAMP2
VDAC1
MS
β-actin
250
150
100
75
50
37
25
B
Supernatant
1 2 3 4 5 6 7 8 9 10 kDa
LAMP2
VDAC1
MS
β-actin
250
150
100
75
50
37
25

Figure 3

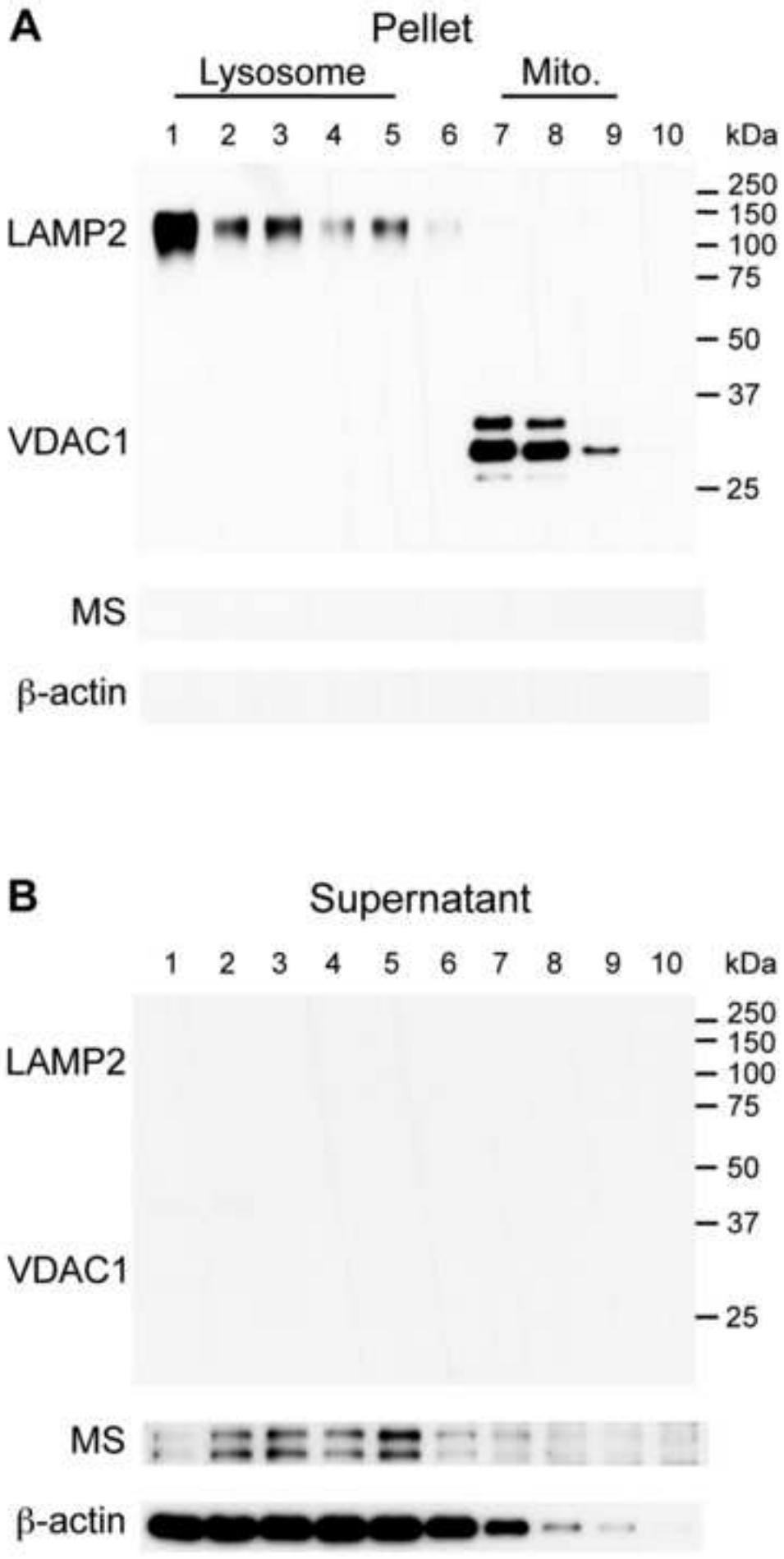
A
Pellet
Lysosome
Mito.
1 2 3 4 5 6 7 8 9 10 kDa
LAMP2
VDAC1
MS
β-actin
250
150
100
75
50
37
25
B
Supernatant
1 2 3 4 5 6 7 8 9 10 kDa
LAMP2
VDAC1
MS
β-actin
250
150
100
75
50
37
25

Figure 4

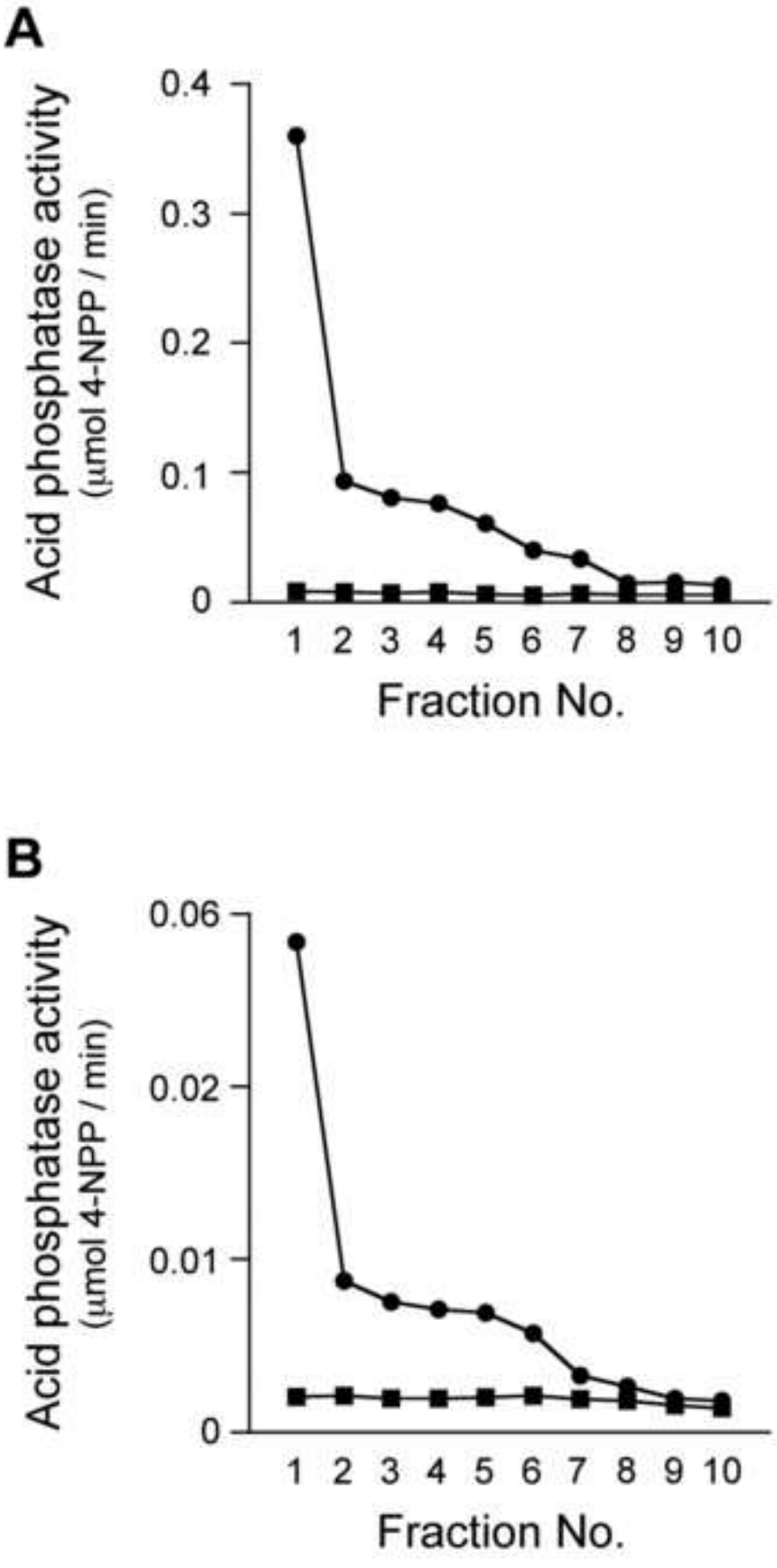
A
Acid phosphatase activity
(μmol 4-NPP / min)
0.4
0.3
0.2
0.1
0
1 2 3 4 5 6 7 8 9 10
Fraction No.
B
Acid phosphatase activity
(μmol 4-NPP / min)
0.06
0.02
0.01
0
1 2 3 4 5 6 7 8 9 10
Fraction No.

Figure 5

A

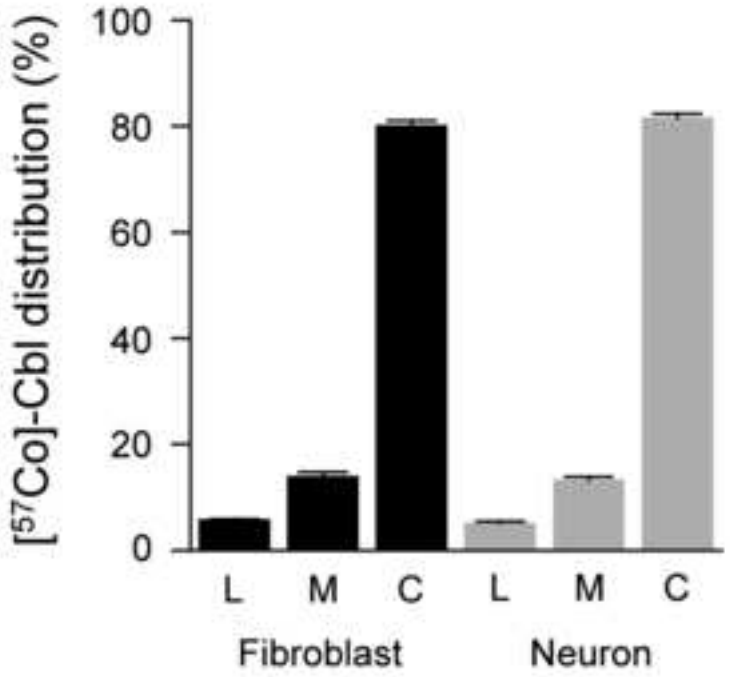

B

HT1080 Fibroblast	Lysosome (cpm)	Mitochondria (cpm)	Cytosol (cpm)
Exp. 1	17 000	39 900	244 000
Exp. 2	19 300	45 400	276 800
Exp. 3	10 600	26 600	135 500

SHSY5Y Neuron	Lysosome (cpm)	Mitochondria (cpm)	Cytosol (cpm)
Exp. 1	3 600	9 900	67 100
Exp. 2	6 200	17 100	96 500
Exp. 3	8 400	19 700	119 300

Figure 6

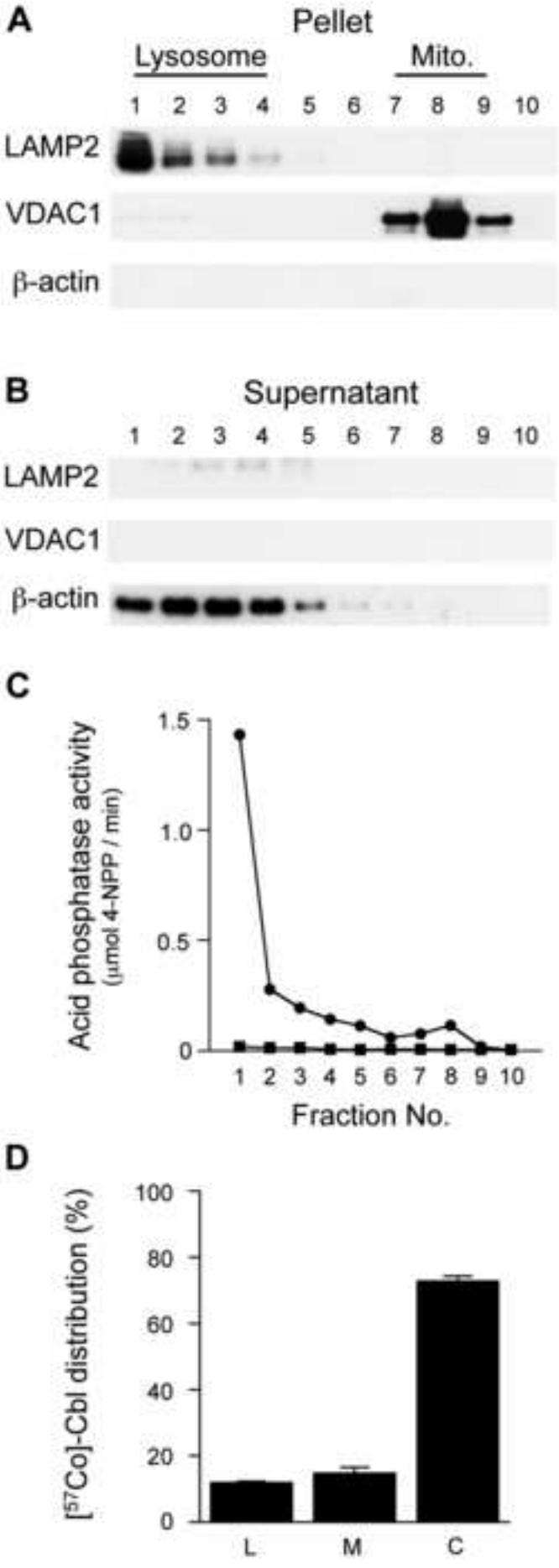
A
Pellet
Lysosome
Mito.
1 2 3 4 5 6 7 8 9 10
LAMP2
VDAC1
β-actin
B
Supernatant
1 2 3 4 5 6 7 8 9 10
LAMP2
VDAC1
β-actin
C
Acid phosphatase activity
(μmol 4-NPP / min)
1.5
1.0
0.5
0
1 2 3 4 5 6 7 8 9 10
Fraction No.
D
[57Co]-Cbl distribution (%)
100
80
60
40
20
0
L
M
C